

2014

# Cancellation of Cellular Responses to Nanoelectroporation by Reversing the Stimulus Polarity

Andrei G. Pakhomov  
*Old Dominion University*

Iurii Semenov  
*Old Dominion University*

Shu Xiao  
*Old Dominion University*

Olga N. Pakhomova  
*Old Dominion University*

Betsy Gregory  
*Old Dominion University*

*See next page for additional authors*

Follow this and additional works at: [https://digitalcommons.odu.edu/bioelectrics\\_pubs](https://digitalcommons.odu.edu/bioelectrics_pubs)

 Part of the [Biochemistry Commons](#), and the [Cancer Biology Commons](#)

---

## Repository Citation

Pakhomov, Andrei G.; Semenov, Iurii; Xiao, Shu; Pakhomova, Olga N.; Gregory, Betsy; and Schoenbach, Karl H., "Cancellation of Cellular Responses to Nanoelectroporation by Reversing the Stimulus Polarity" (2014). *Bioelectrics Publications*. 175.  
[https://digitalcommons.odu.edu/bioelectrics\\_pubs/175](https://digitalcommons.odu.edu/bioelectrics_pubs/175)

## Original Publication Citation

Pakhomov, A. G., Semenov, I., Xiao, S., Pakhomova, O. N., Gregory, B., Schoenbach, K. H., . . . Ibey, B. L. (2014). Cancellation of cellular responses to nanoelectroporation by reversing the stimulus polarity. *Cellular and Molecular Life Sciences*, 71(22), 4431-4441. doi:10.1007/s00018-014-1626-z

---

**Authors**

Andrei G. Pakhomov, Iurii Semenov, Shu Xiao, Olga N. Pakhomova, Betsy Gregory, and Karl H. Schoenbach



Published in final edited form as:

*Cell Mol Life Sci.* 2014 November ; 71(22): 4431–4441. doi:10.1007/s00018-014-1626-z.

## Cancellation of cellular responses to nanoelectroporation by reversing the stimulus polarity

**Andrei G. Pakhomov,**

Frank Reidy Research Center for Bioelectronics, Old Dominion University, 4211 Monarch Way, Suite 300, Norfolk, VA 23508, USA

**Iurii Semenov,**

Frank Reidy Research Center for Bioelectronics, Old Dominion University, 4211 Monarch Way, Suite 300, Norfolk, VA 23508, USA

**Shu Xiao,**

Frank Reidy Research Center for Bioelectronics, Old Dominion University, 4211 Monarch Way, Suite 300, Norfolk, VA 23508, USA

Department of Electrical and Computer Engineering, Old Dominion University, Norfolk, VA 23508, USA

**Olga N. Pakhomova,**

Frank Reidy Research Center for Bioelectronics, Old Dominion University, 4211 Monarch Way, Suite 300, Norfolk, VA 23508, USA

**Betsy Gregory,**

Frank Reidy Research Center for Bioelectronics, Old Dominion University, 4211 Monarch Way, Suite 300, Norfolk, VA 23508, USA

**Karl H. Schoenbach,**

Frank Reidy Research Center for Bioelectronics, Old Dominion University, 4211 Monarch Way, Suite 300, Norfolk, VA 23508, USA

Department of Electrical and Computer Engineering, Old Dominion University, Norfolk, VA 23508, USA

**Jody C. Ullery,**

General Dynamics Information Technology, Fort Sam Houston, San Antonio, TX 78234, USA

**Hope T. Beier,**

Bioeffects Division, 711th Human Performance Wing, Air Force Research Laboratory, Fort Sam Houston, San Antonio, TX 78234, USA

**Sambasiva R. Rajulapati, and**

Department of Electrical and Computer Engineering, Old Dominion University, Norfolk, VA 23508, USA

**Bennett L. Ibey**

Bioeffects Division, 711th Human Performance Wing, Air Force Research Laboratory, Fort Sam Houston, San Antonio, TX 78234, USA

Andrei G. Pakhomov: 2andrei@pakhomov.net; Olga N. Pakhomova: apakhomo@odu.edu

**Abstract**

Nanoelectroporation of biomembranes is an effect of high-voltage, nanosecond-duration electric pulses (nsEP). It occurs both in the plasma membrane and inside the cell, and nanoporated membranes are distinguished by ion-selective and potential-sensitive permeability. Here we report a novel phenomenon of bioeffects cancellation that puts nsEP cardinally apart from the conventional electroporation and electrostimulation by milli- and microsecond pulses. We compared the effects of 60- and 300-ns monopolar, nearly rectangular nsEP on intracellular  $\text{Ca}^{2+}$  mobilization and cell survival with those of bipolar 60 + 60 and 300 + 300 ns pulses. For diverse endpoints, exposure conditions, pulse numbers (1–60), and amplitudes (15–60 kV/cm), the addition of the second phase cancelled the effects of the first phase. The overall effect of bipolar pulses was profoundly reduced, despite delivering twofold more energy. Cancellation also took place when two phases were separated into two independent nsEP of opposite polarities; it gradually tapered out as the interval between two nsEP increased, but was still present even at a 10- $\mu\text{s}$  interval. The phenomenon of cancellation is unique for nsEP and has not been predicted by the equivalent circuit, transport lattice, and molecular dynamics models of electroporation. The existing paradigms of membrane permeabilization by nsEP will need to be modified. Here we discuss the possible involvement of the assisted membrane discharge, two-step oxidation of membrane phospholipids, and reverse transmembrane ion transport mechanisms. Cancellation impacts nsEP applications in cancer therapy, electrostimulation, and biotechnology, and provides new insights into effects of more complex waveforms, including pulsed electromagnetic emissions.

**Keywords**

Electroporation; Electroporeabilization; Cell membrane; Nanosecond pulsed electric field; Bipolar pulses; Ablation

**Introduction**

In living cells, intense electric pulses of nanosecond duration (nsEP) impair the barrier function of membranous structures, including the plasma membrane, endoplasmic reticulum, and mitochondria [1-7]. The downstream effects of nsEP range from cell uptake of membrane-impermeable solutes [8, 9] and transient calcium mobilization [5, 6, 10, 11] to destruction of the cytoskeleton [12], swelling and blebbing [7], and necrotic or apoptotic cell death [1, 2, 13-15]. The membrane defects produced by nsEP have been intensively studied experimentally [7, 16, 17] as well as by molecular dynamics [18-21] and other simulation techniques [22-26], but their exact nature remains elusive.

Most studies agree that such defects represent transient aqueous pores in the phospholipid bilayer, with the effective pore diameter not exceeding 1–1.5 nm (“nanopores”). This pore

size was established both by the selective uptake of smaller dye molecules and ions [8], and by blockage of cell swelling using solutes too large to pass through the pores [7]. The nanopores are remarkably stable, with a lifetime on the order of minutes [8, 13, 16, 17, 27] and show complex conductive properties akin to native ion channels, such as voltage sensitivity, current rectification, and ion selectivity [16, 17]. Mild nsEP stimulation was proposed as a unique method of cell activation that can bypass plasma membrane receptors and channels [5, 6, 10, 28].

The difference between membrane permeabilization by nsEP and the traditional electroporation with longer milli- and microsecond stimuli has been a subject of a continuous debate. Reaching the cell interior and disruption of organelle membranes was introduced theoretically and then confirmed experimentally as the distinctive effect of nsEP [2, 15, 25]. However, longer pulses can also reach the cell interior when the pulse continues after the plasma membrane is already porated [29]. The small pore size is commonly regarded as another attribute of nsEP effects [9, 17, 26], but in fact it is not so specific either. Nanopores can experience thermal and stochastic size fluctuations and coalesce into larger pores [29], whereas longer pulses can produce nanopores as part of mixed-size pore populations or by shrinkage of larger pores [30-34]. The conductive properties of nanopores produced by longer pulses have not been explored in detail (it is difficult to separate them from larger pores), but there is little reason to expect that they will differ from pores formed by nsEP.

These findings suggest a continuum of effects from millisecond down to nanosecond pulse durations, with significant but quantitative rather than qualitative differences. However, in this paper, we counter this judgment by reporting a new phenomenon unique for nsEP, which is the cancellation of bioeffects when one monopolar nsEP is closely followed by a second monopolar nsEP of the opposite polarity. As a result, two such nsEP cause less of an effect than one, and a bipolar nsEP is less efficient than its single phase.

This phenomenon comes in sheer contrast to conventional electroporation where the increase in pulse duration or pulse number is always associated with increased bioeffects. As a rule of thumb, bioeffects are proportional to the time duration when the pulse voltage exceeds a critical level, regardless of the pulse polarity or shape [35]. Hence, a bipolar pulse is always more efficient than a single phase of it, and monopolar pulses are usually compared with bipolar pulses of the equal total duration [36-42]. For different endpoints, the efficiency of bipolar pulses was reported as being similar to monopolar [38, 40-42]; or somewhat higher (because of a larger area of poration [18, 38], reversed direction of electrophoresis [41, 42], or other factors [36, 39]); or somewhat lower (because of reduced electrolytic contamination [37], reversed direction of electrophoresis [41], or other factors [42, 43]). These studies with micro- and millisecond stimuli provided no indication that the second phase of a bipolar pulse may heal or reverse the effect of the first phase.

This study is our second report on the bioeffects of bipolar nsEP. The first one [44] focused specifically on bipolar pulses of the total duration equal to a monopolar pulse (300 + 300 vs. 600 ns). Consistent with the present work, diverse bioassays established a much weaker electroporation effect of the bipolar pulses.

## Materials and methods

### Cell lines

CHO-K1 (Chinese hamster ovary) and U937 (human monocytes) cells were obtained from ATCC (Manassas, VA) and grown in humidified 5 % CO<sub>2</sub> in air in standard culture dishes. CHO cells were propagated in F12 K medium supplemented with 10 % fetal bovine serum, 100 IU/ml penicillin, and 0.1 µg/ml streptomycin. U937 cells were grown in RPMI 1640 medium supplemented with 10 % fetal bovine serum and 2 mM L-glutamine. The media and its components were purchased from Mediatech Cellgro (Herndon, VA) except for the serum (Atlanta Biologicals, Norcross, GA).

### Calcium imaging

The cytosolic free Ca<sup>2+</sup> concentration ([Ca<sup>2+</sup>]<sub>i</sub>) was monitored by time lapse ratiometric fluorescence imaging with Fura-2. The detailed procedures were reported previously [5, 6].

In brief, CHO cells seeded onto glass coverslips and loaded with dye were transferred in a glass-bottomed chamber mounted on an IX71 microscope (Olympus America, Center Valley, PA). The chamber was continually perfused with a physiological solution containing (in mM): 140 NaCl, 5.4 KCl, 1.5 MgCl<sub>2</sub>, 2 CaCl<sub>2</sub>, 10 glucose, and 10 HEPES (pH 7.3, 290–300 mOsm/kg). For Ca<sup>2+</sup>-free conditions, CaCl<sub>2</sub> was replaced with 2 mM Na-EGTA. In some experiments, Ca<sup>2+</sup> was depleted from the endoplasmic reticulum (ER) by preincubation of cells with 10 µM of cyclopiazonic acid (CPA).

Fura-2 was excited alternatively at 340 and 380 nm using a fast wavelength switcher Lambda DG4 (Sutter Instruments, Novato, CA). Emission was measured at 510 nm with a C9100-02 EM CCD camera (Hamamatsu Photonics, Japan) or with an iXon Ultra 897 back-illuminated CCD Camera (Andor Technology, Belfast, UK). [Ca<sup>2+</sup>]<sub>i</sub> was calculated from Fura-2 emission ratio with the help of Metafluor v.7.5 software (Molecular Devices, Sunnyvale, CA). Ca<sup>2+</sup> measurements typically began 1 min prior to nsEP exposure at a rate of 5 or 10 datapoints/s and continued for 3–5 min afterwards. Each cell or group of cells was exposed only once, to a single nsEP.

Fura-2 pentapotassium salt, Fura-2/AM, calcium calibration buffer kit, and Pluronic F-127 (20 % solution in DMSO) were purchased from Life Technologies (Grand Island, NY). CPA was from Tocris Bioscience (Minneapolis, MN). Other chemicals were from Sigma–Aldrich (St. Louis, MO).

### Microscope-based nsEP exposure setup and dosimetry

Except for using both the bipolar and monopolar pulse generators, the exposure procedures were the same as described previously [5, 6]. Pulses were delivered to selected cells on a coverslip with a pair of 0.1-mm-diameter tungsten rods. With the help of an MPC-200 manipulator (Sutter, Novato, CA), the rods were positioned precisely at 30 µm above the coverslip surface so that selected cells were in the middle of the 0.175-mm gap between their tips. The electric field at the location of the cells was determined by a 3D simulation with a finite-element Maxwell equation solver Amaze 3D (Field Precision, Albuquerque,

NM). nsEP were triggered externally and synchronized with image acquisition by a TTL pulse protocol using a Digidata 1440A board and Clampex v. 10.2 software (Molecular Devices). The exact pulse shapes and amplitudes were captured and measured with a TDS 3052 oscilloscope (Tektronix, Beaverton, OR). Hereinafter in this paper, the reported amplitude of bipolar pulses is the amplitude of the first phase (the peak-to-peak amplitude is twofold higher).

Monopolar 60-ns pulses were produced in a Blumlein line-based generator described previously [6]. Bipolar 120-ns pulses (60 ns per phase) were produced by a bidirectional pulse-forming line that utilized MOSFET switches (IXYSRF, DE275-102N06A) and 12-m length of a 50-Ohm cable [45]. The circuitry to produce 600-ns bipolar pulses (300 + 300 ns) was based on a full-bridge voltage-source inverter (VSI) [46]. Four MOS-FETs (IXYS, IXFB38N100Q2, 1 kV) were used. Either the top or the bottom switch of each leg was turned on to allow one polarity of the pulse generated. The timing was controlled by a model DG535 Digital Delay Generator (Stanford Research Systems, Sunnyvale, CA), which generated two control pulses to trigger the diagonal switches in VSI sequentially. A dead time of at least 5 ns was given between the control pulses. The two pulses could be separated by a predetermined delay set by the delay generator. The full-bridge VSI amplified the pulses up to 1 kV in a bipolar fashion. To prevent a possible short circuit, a 20-Ohm high-power resistor (2 W) was placed in series with the electrodes to limit the current and protect the switches. Two high-voltage probes (P5100, Tektronix) were used to measure the voltages at the electrodes with respect to the ground; the difference of the two voltages was the voltage across the exposure electrodes.

With this system, applying just one polarity and physically disconnecting the second polarity input produced a monopolar 300-ns pulse. Applying both polarities with a zero delay produced a bipolar 600-ns pulse (300 ns per phase), and increasing the delay resulted in the delivery of two 300-ns pulses of the opposite polarities. Importantly, the pulse shapes and amplitudes did not depend on the delay or the presence of the second phase. Representative monopolar and bipolar pulse shapes are shown in Figs. 1 and 5.

### **nsEP exposure of cell suspensions and the cell viability assay**

For cell survival analysis, suspensions of CHO and U937 cells were exposed electroporation cuvettes with 1-mm gap (BioSmith Biotech, San Diego, CA). The general protocols were described previously [13, 47, 48]. Cells were suspended in the respective full growth medium (with serum and other supplements) at  $1.5 \times 10^6$  cells/ml, aliquoted at 140  $\mu$ l per cuvette, and exposed to nsEP within several minutes. Different exposure regimens were alternated in a random manner.

After exposure, 100  $\mu$ l of nsEP-treated cells were collected into a microcentrifuge tube and mixed with 200  $\mu$ l of respective medium. The sample was aliquoted into three wells of a black-wall 96-well plate (100  $\mu$ l/well) and moved into the incubator. At 23 h after the exposure, 10  $\mu$ l of the Presto Blue reagent (Life Technologies, Grand Island, NY) was added to each well and incubation continued for 1 h at 37 °C. The plates were read with a Synergy 2 microplate reader (BioTEK, Winooski, VT), with ex./em. settings at 530/590 nm. The data

were corrected for background fluorescence by subtracting values for the wells that contained culture medium without cells.

The triplicate data were averaged, corrected for the background, and considered as a single experiment. The data were presented as mean  $\pm$  SE for  $n$  independent experiments.

Monopolar 60- or 300-ns pulses were generated by 10-Ohm pulse-forming lines consisting of five 50-Ohm cables (6 m in length for 60 ns, 30 m for 300 ns) [49, 50]. To generate bipolar pulses (60 + 60 and 300 + 300 ns), we used bi-directional pulse-forming lines described elsewhere [45, 51]. The cable length was 12 and 60 m for bipolar pulses of 120 and 600 ns, respectively. All these devices utilized an atmospheric pressure spark gap as a switch, so the pulse repetition rate could be controlled only approximately by the rate of network charging. We utilized the pulse rates of about 1 Hz for 60-ns pulses, and 0.2 Hz for 300-ns pulses. The number of pulses delivered to the sample was controlled manually.

## Results

### Reversing the polarity inhibits Ca<sup>2+</sup> activation and cell killing by 60-ns pulses

Recently, we reported that monopolar nsEP evoke Ca<sup>2+</sup> transients even in CHO cells that do not express voltage-activated Ca<sup>2+</sup> channels, and that the removal of extracellular Ca<sup>2+</sup> reduces but does not eliminate the response [5, 6, 52]. Ca<sup>2+</sup> mobilization resulted from a short-lived and fully reversible nanoelectroporation of both the cell membrane and ER, combined with calcium-induced calcium release (CICR) at higher stimulus intensities. At the highest nsEP amplitude of 30 kV/cm, cytosolic free Ca<sup>2+</sup> concentration ([Ca<sup>2+</sup>]<sub>i</sub>) in CHO cells increased abruptly and peaked at 1–3  $\mu$ M within 20–40 s (Fig. 1a).

Bipolar nsEP (30 ns at each polarity) were strikingly less efficient. The response to a single nsEP was just marginally above the baseline, and did not exceed 0.2–0.3  $\mu$ M even with multiple stimuli (Fig. 1b–d). The simplest explanation for this finding was that 30 ns falls at or below some critical pulse duration needed for Ca<sup>2+</sup> activation. To test it out, both phases of the bipolar nsEP were increased to 60 ns; thus, its first phase was made identical to the entire monopolar 60-ns pulse (Fig. 1f). However, even 60 + 60 ns bipolar pulses (Fig. 1e) were far less efficient than monopolar 60-ns stimuli, and this observation held true for different stimulus amplitudes (Fig. 2, left panel). Hence, it was not the pulse or phase duration per se but the bipolar shape of the pulse that caused the reduction of the effect. This reduction took place despite delivering twofold greater energy by the bipolar stimuli. Since a bipolar pulse is essentially a succession of two monopolar pulses of opposite polarities, one can say that the addition of the second pulse cancels the effect of the first one.

We further checked if this paradoxical response to bipolar pulses was unique for different physiological components of the Ca<sup>2+</sup> response. In the absence of extra-cellular Ca<sup>2+</sup>, the response was completely determined by Ca<sup>2+</sup> efflux from the ER and its possible amplification by CICR. In the presence of extracellular Ca<sup>2+</sup>, but after its depletion from the ER with CPA, the response was entirely determined by Ca<sup>2+</sup> influx from the outside [6]. Under all tested conditions, monopolar 60-ns pulses were profoundly more efficient than 60 + 60 ns bipolar ones (Fig. 2, center and right panels).



The next question was whether this finding was unique for  $\text{Ca}^{2+}$  activation by nsEP. We compared the effects of mono- and bipolar nsEP (60 and 60 + 60 ns, respectively) using a more integrative and delayed endpoint, namely the 24-hr cell survival after high-intensity nsEP trains. These experiments utilized a different nsEP delivery procedure (exposure of cell suspensions in electroporation cuvettes) and employed specialized nsEP generators; we also tested two different cell lines. Irrespective of all the differences, monopolar pulses were again proven significantly more efficient than bipolar ones, and incurred up to 5-6-fold more cell death (Fig. 3).

### Effects of longer nsEP and of phase separation

The cancellation of nsEP effects by reversing the electric field direction is the opposite to the experience with longer electric pulses [35-38, 40-43], suggesting different mechanisms of action. Increasing the pulse duration from the nano- into micro- and millisecond range should eventually lead to a transition from cancellation to enhancement of bioeffects. Finding this transition point may help to identify the mechanisms specific for nsEP bioeffects, but absent or masked in longer pulse treatments.

Therefore, we increased the pulse duration fivefold, with the anticipation that the transition point will already be reached. However, the experiments proved it wrong, and the difference in cell killing by monopolar 300-ns pulses and bipolar 300 + 300-ns pulses remained as profound as with the shorter stimuli (Fig. 4).

Instead of testing still longer pulse durations (which would require separate pulse generators for each), we further looked for the transition point by applying two monopolar nsEP of opposite polarities at the intervals from zero (a bipolar pulse) to 10  $\mu\text{s}$  (Fig. 5, inset). Similar to the cytotoxicity findings, the bipolar 300 + 300-ns pulses were very inefficient in activating the cytosolic  $\text{Ca}^{2+}$  (Fig. 5). The canceling effect of the second pulse gradually diminished as the interval between pulses increased. As the interval reached 10  $\mu\text{s}$ , the effect of two pulses became about the same as that of a single pulse.

## Discussion

This study is the first report of cancellation of nsEP effects by reversing the electric field direction. This phenomenon was established using diverse endpoints, exposure conditions, and cell lines. By comparing our data with published findings with longer pulses [35-38, 40-43], we conclude that the cancellation is specific to nanosecond stimuli (perhaps also including the lower microsecond range).

The canceling effect has not been predicted by any biophysical models of electroporation. The mere fact that nsEP effects can be cancelled after the pulse had already been applied changes the existing electroporation paradigm, suggesting that the primary action of nsEP continues long after the duration of the pulse. In this case, the second nsEP of the opposite polarity stops this action earlier than it would cease on its own. The only alternative explanation is that the second pulse can actually undo (heal) the damage already incurred by the first pulse.

Neither of these features was observed in experiments with longer electric pulses. Below we discuss several mechanisms that could be responsible for the peculiarity of nsEP effects.

### Assisted membrane discharge

The charging time constant for a typical mammalian cell is about 1  $\mu\text{s}$  [29], and it should be similar for the passive discharge of undamaged membranes. Although electroporated membranes discharge faster, for a certain time interval after nsEP they remain above the critical voltage [35] where the pore formation or expansion continues (Fig. 6a). Changing the polarity of the external electric field will assist the discharge, thereby reducing the time above the critical voltage (Fig. 6b). The membrane re-polarization starts at the already-high membrane potential and therefore does not reach the critical potential of the opposite polarity.

Thus, the E-field reversal can speed up the membrane discharge and thereby reduce nsEP effects. However, the intervals at which we still observed cancellation (up to 10  $\mu\text{s}$ ) appear far longer than any estimates for the discharge time of electroporated membranes.

Alternatively, the data may indicate that the estimates based on electrical cell models are oversimplified and do not reflect actual living cell parameters.

### Electropermeabilization of membranes as a two-step chemical process

With long electric pulses, reversing the polarity half-way through the pulse duration decreased the yield of electrochemical products and reduced electrode corrosion [37, 53, 54]. This effect is caused by the alternation of reduction and oxidation at the electrode surface as the E-field is reversed. This explanation may also apply to bioeffects of bipolar pulses if electroporation is an electrochemical process, at least in part.

Electroporation is thought to reflect the breakdown of the phospholipid bilayer by the excessive membrane potential [2, 25, 55], but other mechanisms have been considered as well. Cell survival studies suggested generation of reactive oxygen species (ROS) by nsEP, and the depletion of oxygen reduced cell killing [56, 57]. Changes in the whole-cell conductance and cell morphology triggered by nsEP are similar to those of a free radical-induced necrosis [8, 17, 58]. ROS formation was demonstrated in nsEP-treated media even in the absence of cells [59]. A recently proposed hypothesis separates the short-lived electroporation of the membrane from its long-lasting permeabilization due to the oxidation of phospholipids [60].

Membrane electropermeabilization by ROS would include ROS formation as a first step, and oxidation of the membrane as a next step. The first step can be reversed by the reversal of the E-field, similarly to other electrochemical effects [37, 53, 54], which will prevent the membrane oxidation and cancel downstream bioeffects. The E-field reversal will have no protective effect if it happens too late, when the oxidation has already occurred; that is why canceling of bioeffects is specific to nsEP and was not observed with long pulses. A number of reactive species, such as singlet oxygen [61], have the lifetime of several microseconds, which matches the time interval when the effects of the first nsEP still can be cancelled (Fig. 4).

At present, the oxidation hypothesis of electropermeabilization still requires experimental proof, and protective effects of ROS scavengers in nsEP-treated cells have not been demonstrated.

### Reverse electrophoretic transport

Opening of transmembrane aqueous pores by electroporation results in two types of molecular transfer, electrophoretic and diffusional. The electrophoretic transfer (drift) occurs only during the pulse and may move ions even against the concentration gradient. If some ions (e.g.,  $\text{Ca}^{2+}$ ) enter the cell driven by the electric field and do not have enough time to diffuse away from the membrane, the prompt reversal of the field may push them back out of the cell. Thus, the second phase of a bipolar pulse may undo the transmembrane ion transfer produced by the first phase, and thereby cancel the downstream bioeffects.

If membrane pores remain open long after nsEP, the drift will be overwhelmed by the diffusion [22]. However, if these pores close within microseconds, as indicated by pulse probe measurements [62], or even within nanoseconds, as predicted by molecular dynamics models [63], or shrink significantly, the electrophoretic transport may dominate. Identifying the correct scenario is critical for quantitative predictions of the electroporation-mediated molecular delivery. Modeling of  $\text{Ca}^{2+}$  drift based on the experimental data with mono- and bipolar 60- and 300-ns pulses will be presented in a separate paper.

### Broader impact and implications of findings with bipolar pulses

Our findings show that nsEP shape may be just as important in determining bioeffects as its amplitude or duration. Perfectly trapezoidal nsEP are difficult to deliver to biological samples, and “tails” of either the same or reverse polarity as the main pulse are common. Even for the small tail amplitude, the possible canceling impact should be taken into account. As an example, Beebe and coauthors [64] reported an important finding that a long risetime decreased intracellular effects and cell killing by 600-ns pulses. However, the risetime was made longer by adjusting the load impedance, which also generated a reverse polarity tail that could be responsible for the reduced effects.

Trains of short pulses of alternating polarity are used for tumor ablation by so-called high-frequency irreversible electroporation, or H-FIRE [65, 66]. Alternating the polarity helps to reduce unwanted muscle contractions while still achieving tumor ablation. The theoretical study [66] predicted that submicrosecond bipolar pulses are best suited to penetrate epithelial layers with minimal thermal effect and to electroporate the underlying cells. However, this analysis extrapolated the knowledge with longer pulses [35] into the nsEP range, and it may be misleading without considering the canceling phenomena.

Our findings can also impact the understanding of bioeffects of radiated electromagnetic pulses, including ultrawide band and microwave emissions. The emitted pulses are inherently associated with the E-field reversals, which could be responsible for their low biological efficiency. Indeed, even the most powerful radiated pulses ever tested had little or no biological effect except for trivial heating [67-69]. This idea is also supported by a study that compared electroporation effects of conductively- and capacitively coupled 1.6-ns pulses, and observed no effects of the latter [70]. The capacitive coupling has necessarily

transformed the monopolar pulse shape into a bipolar one, and can be regarded as a simple model for radiated pulses.

In conclusion, we expect that understanding the effects of bipolar pulses will help to develop more precise tools for deliberate manipulation of biological functions, including molecular delivery into living cells and targeted permeabilization of intracellular organelles.

## Acknowledgments

This work was supported by funds from the Air Force Surgeon General's Office, Medical Research Program (to B.L.I.) AFOSR LRIR 13RH08COR (to B.L.I.), and by a National Institutes of Health grant R01GM088303 (to A.G.P.).

## References

1. Beebe SJ, Fox PM, Rec LJ, Willis EL, Schoenbach KH. Nanosecond, high-intensity pulsed electric fields induce apoptosis in human cells. *Faseb J*. 2003; 17(11):1493–1495. [PubMed: 12824299]
2. Schoenbach KS, Hargrave B, Joshi RP, Kolb J, Osgood C, Nuccitelli R, Pakhomov AG, Swanson J, Stacey M, White JA, Xiao S, Zhang J, Beebe SJ, Blackmore PF, Buescher ES. Bioelectric effects of nanosecond pulses. *IEEE Trans Dielectr Electr Insul*. 2007; 14(5):1088–1109.
3. Napotnik TB, Wu YH, Gundersen MA, Miklavcic D, Vernier PT. Nanosecond electric pulses cause mitochondrial membrane permeabilization in Jurkat cells. *Bioelectromagnetics*. 2012; 33:257–264.10.1002/bem.20707 [PubMed: 21953203]
4. White JA, Blackmore PF, Schoenbach KH, Beebe SJ. Stimulation of capacitative calcium entry in HL-60 cells by nanosecond pulsed electric fields. *J Biol Chem*. 2004; 279(22):22964–22972. [PubMed: 15026420]
5. Semenov I, Xiao S, Pakhomova ON, Pakhomov AG. Recruitment of the intracellular  $Ca^{2+}$  by ultrashort electric stimuli: the impact of pulse duration. *Cell Calcium*. 2013; 54(3):145–150.10.1016/j.ceca.2013.05.008 [PubMed: 23777980]
6. Semenov I, Xiao S, Pakhomov A. Primary pathways of intracellular  $Ca^{2+}$  mobilization by nanosecond pulsed electric field. *Biochim Biophys Acta*. 2013; 3:981–989.10.1016/j.bbame.2012.11.032 [PubMed: 23220180]
7. Nesin OM, Pakhomova ON, Xiao S, Pakhomov AG. Manipulation of cell volume and membrane pore comparison following single cell permeabilization with 60- and 600-ns electric pulses. *Biochim Biophys Acta*. 2011; 3:792–801. [PubMed: 21182825]
8. Bowman AM, Nesin OM, Pakhomova ON, Pakhomov AG. Analysis of plasma membrane integrity by fluorescent detection of  $Tl^{+}$  uptake. *J Membr Biol*. 2010; 236(1):15–26.10.1007/s00232-010-9269-y [PubMed: 20623351]
9. Vernier PT, Sun Y, Gundersen MA. Nanoelectropulsed driven membrane perturbation and small molecule permeabilization. *BMC Cell Biol*. 2006; 7:37. [PubMed: 17052354]
10. Craviso GL, Choe S, Chatterjee I, Vernier PT. Modulation of intracellular  $Ca^{2+}$  levels in chromaffin cells by nanoelectropulses. *Bioelectrochemistry*. 2012; 87:244–252.10.1016/j.bioelechem.2011.11.016 [PubMed: 22197468]
11. Vernier PT, Sun Y, Marcu L, Salem S, Craft CM, Gundersen MA. Calcium bursts induced by nanosecond electric pulses. *Biochem Biophys Res Commun*. 2003; 310:286–295. [PubMed: 14521908]
12. Berghofer T, Eing C, Flickinger B, Hohenberger P, Wegner LH, Frey W, Nick P. Nanosecond electric pulses trigger actin responses in plant cells. *Biochem Biophys Res Commun*. 2009; 387(3):590–595.10.1016/j.bbrc.2009.07.072 [PubMed: 19619510]
13. Ibey BL, Pakhomov AG, Gregory BW, Khorokhorina VA, Roth CC, Rassokhin MA, Bernhard JA, Wilmink GJ, Pakhomova ON (2010) Selective cytotoxicity of intense nanosecond-duration electric pulses in mammalian cells. *Biochim Biophys Acta*. 1800; 11:1210–1219.10.1016/j.bbagen.2010.07.008

14. Pakhomova ON, Gregory BW, Semenov I, Pakhomov AG. Two modes of cell death caused by exposure to nanosecond pulsed electric field. *PLoS ONE*. 2013; 8(7):e70278.10.1371/journal.pone.0070278 [PubMed: 23894630]
15. Ren W, Beebe SJ. An apoptosis targeted stimulus with nanosecond pulsed electric fields (nsPEFs) in E4 squamous cell carcinoma. *Apoptosis*. 2011; 16(4):382–393.10.1007/s10495-010-0572-y [PubMed: 21213047]
16. Pakhomov AG, Bowman AM, Ibey BL, Andre FM, Pakhomova ON, Schoenbach KH. Lipid nanopores can form a stable, ion channel-like conduction pathway in cell membrane. *Biochem Biophys Res Commun*. 2009; 385(2):181–186.10.1016/j.bbrc.2009.05.035 [PubMed: 19450553]
17. Pakhomov, AG.; Pakhomova, ON. Nanopores: a distinct transmembrane passageway in electroporated cells. In: Pakhomov, AG.; Miklavcic, D.; Markov, MS., editors. *Advanced electroporation techniques in biology in medicine*. CRC Press; Boca Raton: 2010. p. 178-194.
18. Vernier PT, Levine ZA, Wu YH, Joubert V, Ziegler MJ, Mir LM, Tieleman DP. Electroporating fields target oxidatively damaged areas in the cell membrane. *PLoS ONE*. 2009; 4(11):e7966.10.1371/journal.pone.0007966 [PubMed: 19956595]
19. Ho MC, Casciola M, Levine ZA, Vernier PT. Molecular dynamics simulations of ion conductance in field-stabilized nanoscale lipid electropores. *J Phys Chem B*. 2013 epub ahead of print. 10.1021/jp401722g
20. Tokman M, Lee JH, Levine ZA, Ho MC, Colvin ME, Vernier PT. Electric field-driven water dipoles: nanoscale architecture of electroporation. *PLoS ONE*. 2013; 8(4):e61111.10.1371/journal.pone.0061111 [PubMed: 23593404]
21. Delemotte L, Tarek M. Molecular dynamics simulations of lipid membrane electroporation. *J Membr Biol*. 2012; 245(9):531–543.10.1007/s00232-012-9434-6 [PubMed: 22644388]
22. Smith KC, Weaver JC. Transmembrane molecular transport during versus after extremely large, nanosecond electric pulses. *Biochem Biophys Res Commun*. 2011; 412(1):8–12.10.1016/j.bbrc.2011.06.171 [PubMed: 21756883]
23. Smith KC, Weaver JC. Active mechanisms are needed to describe cell responses to submicrosecond, megavolt-perimeter pulses: cell models for ultrashort pulses. *Biophys J*. 2008; 95(4):1547–1563. [PubMed: 18408042]
24. Joshi RP, Schoenbach KH. Mechanism for membrane electroporation irreversibility under high-intensity, ultrashort electrical pulse conditions. *Phys Rev E: Stat Nonlin Soft Matter Phys*. 2002; 66(5 Pt 1):052901. [PubMed: 12513540]
25. Pakhomov, AG.; Miklavcic, D.; Markov, MS., editors. *Advanced electroporation techniques in biology in medicine*. CRC Press; Boca Raton: 2010.
26. Gowrishankar TR, Weaver JC. Electrical behavior and pore accumulation in a multicellular model for conventional and supra-electroporation. *Biochem Biophys Res Commun*. 2006; 349(2):643–653. [PubMed: 16959217]
27. Pakhomov AG, Kolb JF, White JA, Joshi RP, Xiao S, Schoenbach KH. Long-lasting plasma membrane permeabilization in mammalian cells by nanosecond pulsed electric field (nsPEF). *Bioelectromagnetics*. 2007; 28:655–663. [PubMed: 17654532]
28. Craviso GL, Choe S, Chatterjee P, Chatterjee I, Vernier PT. Nanosecond electric pulses: a novel stimulus for triggering  $Ca^{2+}$  nflux into chromaffin cells via voltage-gated  $Ca^{2+}$  channels. *Cell Mol Neurobiol*. 2010; 30(8):1259–1265.10.1007/s10571-010-9573-1 [PubMed: 21080060]
29. Esser AT, Smith KC, Gowrishankar TR, Vasilkoski Z, Weaver JC. Mechanisms for the intracellular manipulation of organelles by conventional electroporation. *Biophys J*. 2010; 98(11):2506–2514. [PubMed: 20513394]
30. Serpersu EH, Kinoshita K Jr, Tsong TY. Reversible and irreversible modification of erythrocyte membrane permeability by electric field. *Biochim Biophys Acta*. 1985; 812(3):779–785. [PubMed: 3970906]
31. Kinoshita K Jr, Tsong TT. Hemolysis of human erythrocytes by transient electric field. *Proc Natl Acad Sci USA*. 1977; 74(5):1923–1927. [PubMed: 266714]
32. Kinoshita K Jr, Tsong TY. Formation and resealing of pores of controlled sizes in human erythrocyte membrane. *Nature*. 1977; 268(5619):438–441. [PubMed: 895849]

33. Saulis G. Kinetics of pore disappearance in a cell after electroporation. *Biomed Sci Instrum.* 1999; 35:409–414. [PubMed: 11143387]
34. Saulis G, Venslauskas MS, Naktinis J. Kinetics of pore resealing in cell membranes after electroporation. *Bioelectrochem Bioenerg.* 1991; 26:1–13.
35. Kotnik T, Pucihar G, Rebersek M, Miklavcic D, Mir LM. Role of pulse shape in cell membrane electropermeabilization. *Biochim Biophys Acta.* 2003; 1614(2):193–200. S0005273603001731. [PubMed: 12896812]
36. Kotnik T, Mir LM, Flisar K, Puc M, Miklavcic D. Cell membrane electropermeabilization by symmetrical bipolar rectangular pulses. part I. Increased efficiency of permeabilization. *Bioelectrochemistry.* 2001; 54(1):83–90. S1567-5394(01)00114-1. [PubMed: 11506978]
37. Kotnik T, Miklavcic D, Mir LM. Cell membrane electropermeabilization by symmetrical bipolar rectangular pulses part II. Reduced electrolytic contamination. *Bioelectrochemistry.* 2001; 54(1): 91–95. S1567-5394(01)00115-3. [PubMed: 11506979]
38. Tekle E, Astumian RD, Chock PB. Electroporation by using bipolar oscillating electric-field—an improved method for DNA transfection of NIH 3T3 Cells. *Proc Natl Acad Sci USA.* 1991; 88(10): 4230–4234. 10.1073/pnas.88.10.4230 [PubMed: 2034667]
39. Moroz VV, Bogushevich MS, Chernysh AM, Kozlova EK, Sharakshane AS. Effect of defibrillation pulses of different shapes on biomembranes: experimental study. *Bull Exp Biol Med.* 2004; 137(2):120–123. 10.1023/B:Bebm.0000028118.86481.F6 [PubMed: 15273753]
40. Tovar O, Tung L. Electroporation of cardiac cell-membranes with monophasic or biphasic rectangular pulses. *Pace.* 1991; 14(11):1887–1892. 10.1111/j.1540-8159.1991.tb02785.x [PubMed: 1721194]
41. Faurie C, Rebersek M, Golzio M, Kanduser M, Escoffre JM, Pavlin M, Teissie J, Miklavcic D, Rols MP. Electro-mediated gene transfer and expression are controlled by the life-time of DNA/membrane complex formation. *J Gene Med.* 2010; 12(1):117–125. 10.1002/jgm.1414 [PubMed: 19941315]
42. Faurie C, Phez E, Golzio M, Vossen C, Lesbordes JC, Delteil C, Teissie J, Rols MP. Effect of electric field vectoriality on electrically mediated gene delivery in mammalian cells. *Biochim Biophys Acta.* 2004; 1665(1–2):92–100. 10.1016/j.bbamem.2004.06.018 [PubMed: 15471575]
43. de Oliveira PX, Bassani RA, Bassani JW. Lethal effect of electric fields on isolated ventricular myocytes. *IEEE Trans Biomed Eng.* 2008; 55(11):2635–2642. 10.1109/TBME.2008.2001135 [PubMed: 18990634]
44. Ibey BL, Ullery JC, Pakhomova ON, Roth CC, Semenov I, Beier HT, Tarango M, Xiao S, Schoenbach KH, Pakhomov AG. Bipolar nanosecond electric pulses are less efficient at electropermeabilization and killing cells than monopolar pulses. *Biochem Biophys Res Commun.* 2014; 443(2):568–573. 10.1016/j.bbrc.2013.12.004 [PubMed: 24332942]
45. Rajulapati, SR.; Husain, FA.; Ananthapadmanabha, SB.; Schoenbach, KH.; Xiao, S. Nanosecond biphasic pulse generators for biomedical applications. Pulsed power conference (PPC), 19th IEEE; 16–21 June 2013; 2013. p. 1–4.
46. Rashid, MH., editor. *Power electronics handbook : devices, circuits, and applications handbook.* 3. Elsevier; Burlington: 2011.
47. Pakhomova ON, Gregory BW, Khorokhorina VA, Bowman AM, Xiao S, Pakhomov AG. Electroporation-induced electrosensitization. *PLoS ONE.* 2011; 6(2):e17100. 10.1371/journal.pone.0017100 [PubMed: 21347394]
48. Pakhomova ON, Gregory BW, Pakhomov AG. Facilitation of electroporative drug uptake and cell killing by electrosensitization. *J Cell Mol Med.* 2013; 17(1):154–159. 10.1111/j.1582-4934.2012.01658.x [PubMed: 23305510]
49. Schoenbach KH, Beebe SJ, Buescher ES. Intracellular effect of ultrashort electrical pulses. *Bioelectromagnetics.* 2001; 22(6):440–448. [PubMed: 11536285]
50. Beebe SJ, Fox PM, Rec LJ, Somers K, Stark RH, Schoenbach KH. Nanosecond pulsed electric field (nsPEF) effects on cells and tissues: apoptosis induction and tumor growth inhibition. *IEEE Trans Plasma Sci.* 2002; 30(1):286–292.
51. Smith, PW. *Transient electronics : pulsed circuit technology.* Wiley; New York: 2002.



52. Tolstykh GP, Beier HT, Roth CC, Thompson GL, Payne JA, Kuipers MA, Ibey BL. Activation of intracellular phosphoinositide signaling after a single 600 nanosecond electric pulse. *Bioelectrochemistry*. 2013; 94:23–29.10.1016/j.bioelechem.2013.05.002 [PubMed: 23747521]
53. Roodenburg B, Morren J, Berg HE, de Haan SWH. Metal release in a stainless steel pulsed electric field (PEF) system part I. Effect of different pulse shapes; theory and experimental method. *Innov Food Sci Emerg*. 2005; 6(3):327–336.10.1016/j.ifset.2005.04.006
54. Merrill DR, Bikson M, Jefferys JG. Electrical stimulation of excitable tissue: design of efficacious and safe protocols. *J Neurosci Methods*. 2005; 141(2):171–198.10.1016/j.jneumeth.2004.10.020 [PubMed: 15661300]
55. Neumann, E.; Sowers, AE.; Jordan, CA., editors. *Electroporation and electrofusion in cell biology*. Plenum; New York: 1989.
56. Walker K 3rd, Pakhomova ON, Kolb J, Schoenbach KS, Stuck BE, Murphy MR, Pakhomov AG. Oxygen enhances lethal effect of high-intensity, ultrashort electrical pulses. *Bioelectromagnetics*. 2006; 27(3):221–225. [PubMed: 16342277]
57. Pakhomov AG, Phinney A, Ashmore J, Walker K, Kolb J, Kono S, Schoenbach KS, Murphy MR. Characterization of the cytotoxic effect of high-intensity, 10-ns duration electrical pulses. *IEEE Trans Plasma Sci*. 2004; 32(4):1579–1585.
58. Barros LF, Hermosilla T, Castro J. Necrotic volume increase and the early physiology of necrosis. *Comp Biochem Physiol A Mol Integr Physiol*. 2001; 130(3):401–409. [PubMed: 11913453]
59. Pakhomova ON, Khorokhorina VA, Bowman AM, Rodaite-Riseviciene R, Saulis G, Xiao S, Pakhomov AG. Oxidative effects of nanosecond pulsed electric field exposure in cells and cell-free media. *Arch Biochem Biophys*. 2012; 527(1):55–64.10.1016/j.abb.2012.08.004 [PubMed: 22910297]
60. Breton, M.; Mir, LM. Molecular mechanisms of electroporation/ion/electropermeabilization: evidence for a chemical modification of membrane phospholipids. paper presented at the BioEM2013; Thessaloniki, Greece. 10–14 June 2013; 2013.
61. Rodgers MAJ, Snowden PT. Lifetime of O-2(1delta-G) in liquid water as determined by time-resolved infrared luminescence measurements. *J Am Chem Soc*. 1982; 104(20):5541–5543.10.1021/Ja00384a070
62. Benz R, Zimmermann U. The resealing process of lipid bilayers after reversible electrical breakdown. *Biochim Biophys Acta*. 1981; 640(1):169–178. [PubMed: 7213683]
63. Levine ZA, Vernier PT. Life cycle of an electropore: field-dependent and field-independent steps in pore creation and annihilation. *J Membr Biol*. 2010; 236(1):27–36.10.1007/s00232-010-9277-y [PubMed: 20623350]
64. Beebe SJ, Chen YJ, Sain NM, Schoenbach KH, Xiao S. Transient features in nanosecond pulsed electric fields differentially modulate mitochondria and viability. *PLoS ONE*. 2012; 7(12):e51349.10.1371/journal.pone.0051349 [PubMed: 23284682]
65. Arena CB, Sano MB, Rossmesl JH Jr, Caldwell JL, Garcia PA, Rylander MN, Davalos RV. High-frequency irreversible electroporation (H-FIRE) for non-thermal ablation without muscle contraction. *Biomed Eng Online*. 2011; 10:102.10.1186/1475-925X-10-102 [PubMed: 22104372]
66. Arena CB, Sano MB, Rylander MN, Davalos RV. Theoretical considerations of tissue electroporation with high-frequency bipolar pulses. *IEEE Trans Biomed Eng*. 2011; 58(5):1474–1482.10.1109/TBME.2010.2102021 [PubMed: 21189230]
67. Pakhomov AG, Doyle J, Stuck BE, Murphy MR. Effects of high power microwave pulses on synaptic transmission and long term potentiation in hippocampus. *Bioelectromagnetics*. 2003; 24(3):174–181. [PubMed: 12669300]
68. Pakhomov AG, Gajsek P, Allen L, Stuck BE, Murphy MR. Comparison of dose dependences for bioeffects of continuous wave and high-peak power microwave emissions using gel-suspended cell cultures. *Bioelectromagnetics*. 2002; 23(2):158–167. [PubMed: 11835262]
69. Seaman RL. Effects of exposure of animals to ultra-wideband pulses. *Health Phys*. 2007; 92(6):629–634.10.1097/01.Hp.0000256780.23536.15 [PubMed: 17495665]
70. French DM, Uhler MD, Gilgenbach RM, Lau YY. Conductive versus capacitive coupling for cell electroporation with nanosecond pulses. *J Appl Phys*. 2009; 106(7):074701–074704.10.1063/1.3238245

## Abbreviations

<b>CICR</b>	Calcium-induced calcium release
<b>CPA</b>	Cyclopiazonic acid
<b>ER</b>	Endoplasmic reticulum
<b>NsEP</b>	Nanosecond electric pulse
<b>ROS</b>	Reactive oxygen species



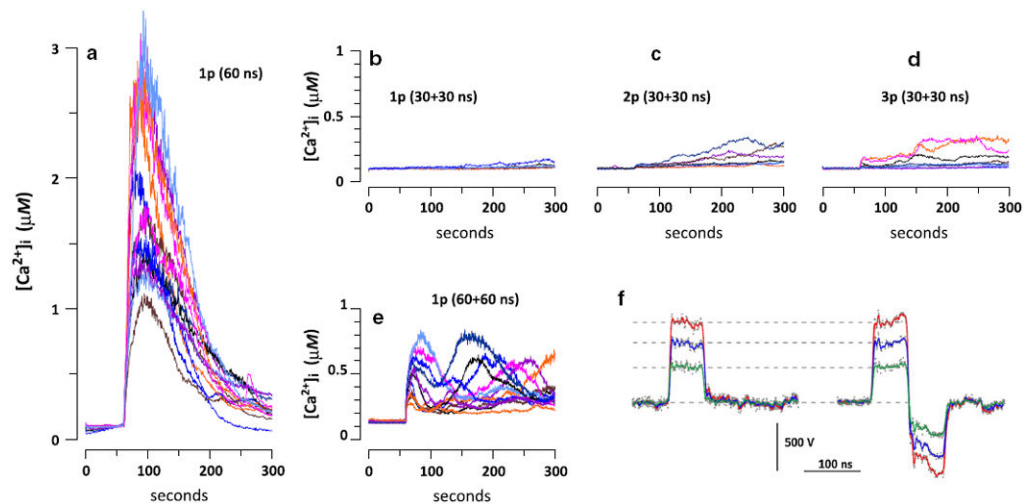


**Fig. 1.**

Calcium transients evoked in CHO cells by a monopolar 60-ns pulse (**a**) and by bipolar pulses at the same amplitude, 30 kV/cm (**b–e**). The duration of bipolar pulses was either 60 ns (30 + 30 ns, **b–d**) or 120 ns (60 + 60 ns, **e**). The stimuli were applied at 60 s into the experiment either as a single pulse (1p), or a train of 2 or 3 pulses (2p and 3p; 50 ms between the pulses). Each panel shows overlapped calcium transients from 8–15 cells. The bath buffer contained 2 mM  $Ca^{2+}$ . All panels are at the same scale. **f** Representative waveforms of mono- and bipolar nsEP (60 and 60 + 60 ns, respectively) at three different amplitudes. Note that the amplitude of bipolar pulses is measured as the amplitude of the first phase

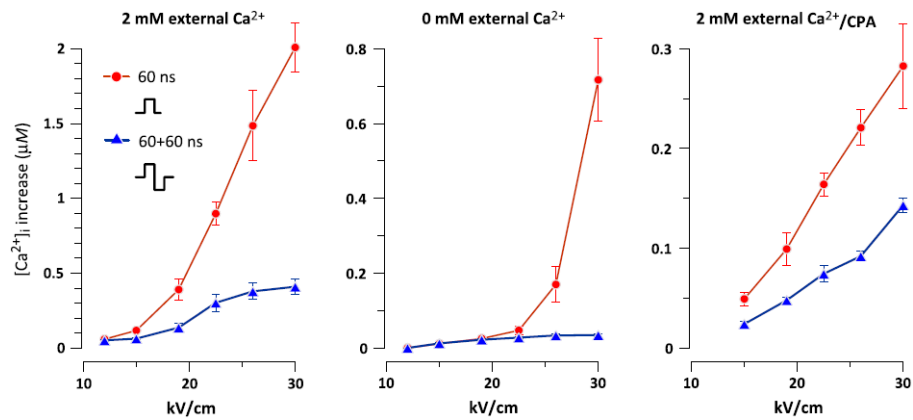


**Fig. 2.** Monopolar stimuli are more efficient at activation of cytosolic  $Ca^{2+}$  from different  $Ca^{2+}$  sources. Plots show the peak amplitude of  $[Ca^{2+}]_i$  in response to monopolar and bipolar stimuli (60 and 60 + 60 ns, respectively). Stimulation was performed in the presence of 2 mM  $Ca^{2+}$  in the medium (*left* and *right panels*) or in its absence (*center*). For the right panel,  $Ca^{2+}$  was depleted from the ER by preincubation with CPA. Mean  $\pm$  SEM,  $N = 6-12$  cells per datapoint. The differences are statistically significant at least at  $p < 0.05$  for all datapoints where the error bars do not overlap (unpaired two-tailed  $t$  test). The mechanisms of  $[Ca^{2+}]_i$  increase included nsEP-induced  $Ca^{2+}$  efflux from the ER and calcium-induced calcium release (*center*), calcium influx from the outside (*right*), and all of the above (*left*)

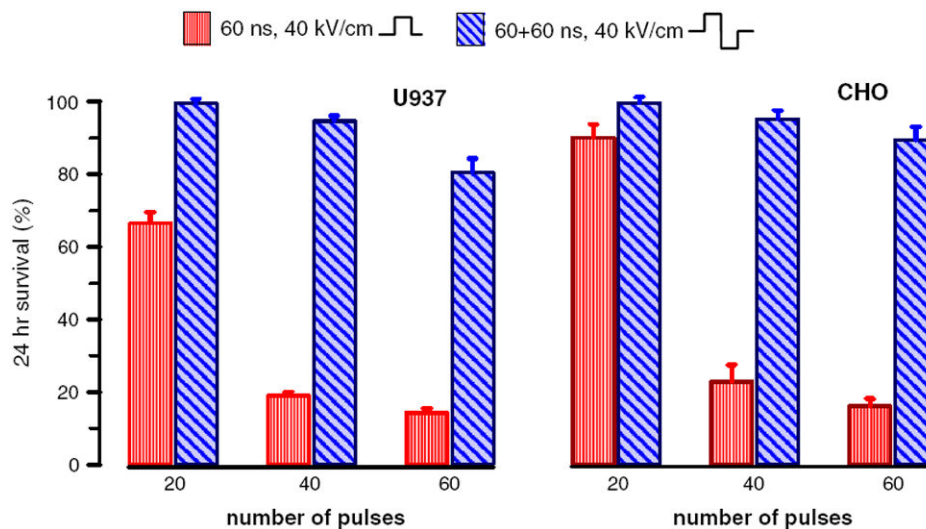


**Fig. 3.** Monopolar 60-ns pulses are more efficient at cell killing than bipolar 60 + 60 ns pulses. The cell death was induced in U937 and CHO cells by trains of 20, 40, or 60 pulses at 40 kV/cm (1 Hz). Cell viability was measured at 24 h after nsEP exposure and expressed as % to sham-exposed parallel controls. Mean  $\pm$  SEM,  $N = 5-7$ . Higher cytotoxic efficiency of monopolar pulses is significant at least at  $p < 0.05$  in all the groups (unpaired two-tailed  $t$  test)

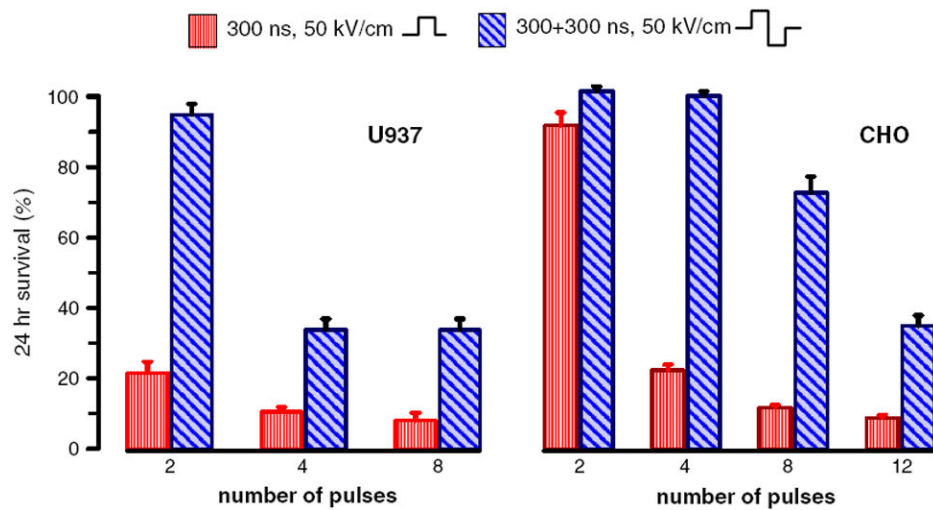


**Fig. 4.** Monopolar 300-ns pulses are more efficient at cell killing than bipolar 300 + 300-ns pulses. U937 and CHO cells were exposed to trains of 2, 4, 8, or 12 pulses at 50 kV/cm (0.2 Hz). Cell viability was measured at 24 h and expressed as % to sham-exposed parallel controls. Mean  $\pm$  SEM,  $N = 3-8$ . Higher cytotoxic efficiency of monopolar pulses is significant at least at  $p < 0.05$  in all the groups (unpaired two-tailed  $t$  test)

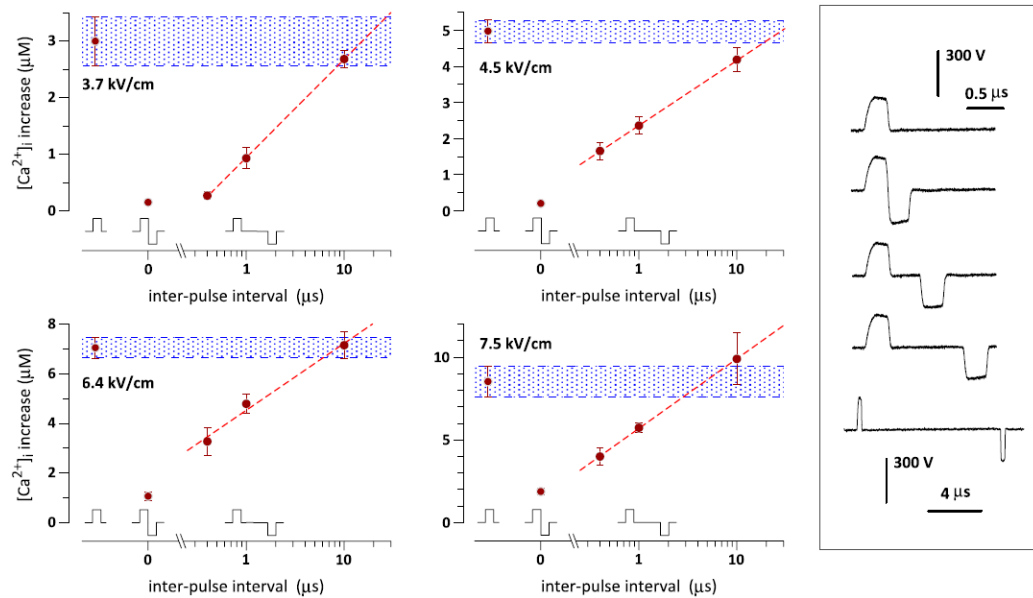


**Fig. 5.**

Cancellation of  $\text{Ca}^{2+}$  response by the application of a second pulse of the opposite polarity. CHO cells were stimulated by a single monopolar 300-ns pulse; or by two 300-ns pulses with the opposite polarities applied immediately one after the other to form a bipolar pulse; or by two 300-ns pulses with different intervals between them. The respective shapes of the stimuli and their amplitudes are shown in the graphs. The mean response to a monopolar pulse ( $\pm$  SEM) at each amplitude is highlighted by the shaded “corridor”. As the opposite polarity pulses get further apart, the amplitude of  $\text{Ca}^{2+}$  response increases as a log function, to match the effect of a monopolar pulse with a separation of about 10  $\mu\text{s}$ . Mean  $\pm$  SEM,  $N=20\text{--}50$  cells for most datapoints. In all the groups, and with the exception of the 10- $\mu\text{s}$  interval, the response to monopolar pulses was significantly higher at least at  $p < 0.02$  (unpaired two-tailed  $t$  test with Dunnett’s correction for multiple groups). *Inset:* Representative waveforms of 300-ns pulses applied as a single pulse (*top*) and in pairs with opposite polarities. The intervals between the pulses in pairs are 0, 0.4, 1, and 10  $\mu\text{s}$  for traces 2–5, respectively

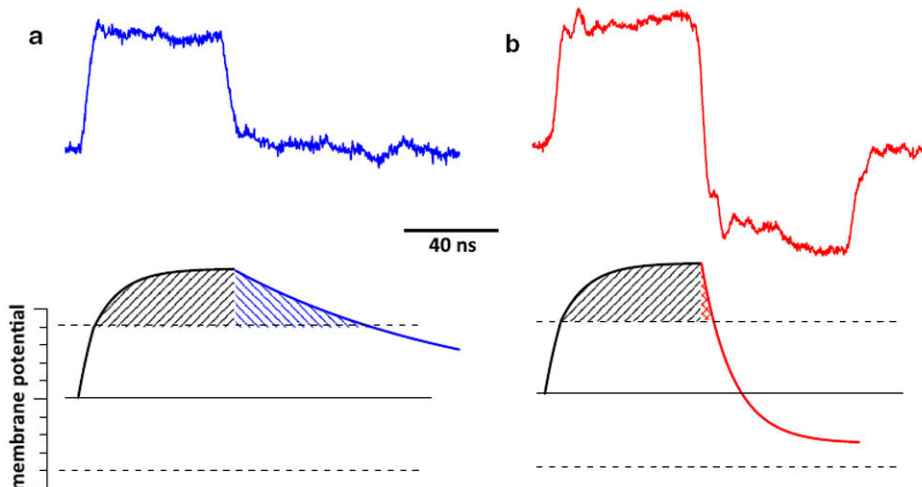


**Fig. 6.** Bipolar pulses may assist cell membrane discharge and reduce the membrane time above the critical voltage. Cell membrane is charged (*bottom*) by a monopolar pulse (**a**, *top*) or a bipolar pulse (**b**, *top*). The membrane voltage (arbitrary units) goes from the baseline (*solid line*) to the critical electroporation voltage (*dashed line*) and above it. The time when the membrane voltage exceeds the critical level is shown by *shading*. The bipolar pulse reduces this time but does not bring the voltage below the negative critical value. See text for details